HHS Public Access

Author manuscript

Nat Methods. Author manuscript; available in PMC 2024 May 08.

Published in final edited form as:

Nat Methods. 2023 August ; 20(8): 1179–1182. doi:10.1038/s41592-023-01911-1.

Expansion Spatial Transcriptomics

Yuhang Fan[1,‡], **Žaneta Andrusivová**[2,‡], **Yunming Wu**[3], **Chew Chai**[1], **Ludvig Larsson**[2], **Mengxiao He**[2], **Liqun Luo**[3], **Joakim Lundeberg**[2,*], **Bo Wang**[1,*]

[1]Department of Bioengineering, Stanford University, Stanford, CA, USA

[2]Department of Gene Technology, KTH Royal Institute of Technology, Science for Life Laboratory, Stockholm, Sweden

[3]Department of Biology, Howard Hughes Medical Institute, Stanford University, Stanford, CA, USA

Abstract

Capture array-based spatial transcriptomics methods have been widely used to resolve gene expression in diverse tissue contexts, however, their spatial resolution is limited by the density of the array. We present Expansion Spatial Transcriptomics (Ex-ST) to overcome this limitation by clearing and expanding tissue prior to capturing the entire polyadenylated transcriptome. This approach allows us to achieve higher spatial resolution which we demonstrate using mouse brain samples.

The spatial distribution of transcripts is essential for understanding cell states and cellular organization in tissues. In recent years, many methods for spatial profiling of gene expression have been developed[1–3]. The first technique that can target the entire transcriptome, introduced by Ståhl *et al.* in 2016, now commercialized by 10x Genomics as the Visium platform, relies on capturing polyadenylated RNA released from tissue sections onto barcoded array surface[4]. Its broad applicability has been demonstrated in various systems to describe developmental processes[5] and profile complex diseases[6,7]. However, its spatial resolution is limited by the density of spatially barcoded arrays. Currently, the spot size is 55 μm with a center-to-center distance of 100 μm, resulting in each spot being occupied by multiple cells.

Here we present Expansion Spatial Transcriptomics (Ex-ST), an approach that allows us to overcome the resolution limit by first expanding samples embedded in a polyelectrolyte matrix before capturing RNA on Visium slides. We applied this method on two mouse

*Correspondence: joakim.lundeberg@scilifelab.se (J.L.) & wangbo@stanford.edu (B.W.).
‡These authors contributed equally to this work.

Author contributions statement

YF, ZA, JL, and BW initiated and designed the project; YF, ZA, YW, and CC performed the experiments; YF and ZA analyzed the data with assistance from YW, L Larsson, and MH; YF, ZA, and BW wrote the paper with input from all other authors; L Luo, JL, and BW provided supervision and guidance.

Competing interests statement

ZA, L Larsson, MH, and JL are scientific consultants for 10x Genomics, which holds IP rights to the ST technology. The remaining authors declare no competing interests.

Code availability

The code used for data analysis and generating figures is available at https://github.com/fyh1221/Expansion_Spatial_Transcriptomics.

brain regions, olfactory bulb and hippocampus, chosen for their well-described anatomically distinct patterns with clear molecular signatures. Our Ex-ST protocol significantly improves the resolution and RNA capture efficiency of the Visium array, enabling us to better resolve cell types and detect rare transcripts.

We took inspiration from expansion microscopy, in which biomolecules are anchored to polyelectrolyte gel matrices that can be expanded to increase imaging resolution[8]. In our Ex-ST protocol (Fig. 1a), a tissue section is embedded in a polyacrylate gel to anchor RNA. After all proteins are digested, the gel undergoes ~2.5 times linear expansion in 0.1× SSC buffer. The expanded gel is stained with DAPI, placed on the Visium capture array where fluorescent images are taken to register nuclei for aligning anatomy and gene expression in later steps. A key design of Ex-ST is the use of two poly-dT probes of different lengths and melting temperatures (MT), with the shorter one (MT ~39°C) anchored in the gel and the longer one (MT > 55°C) spatially barcoded on the Visium slides. This allows us to use heat (45°C for 30 min) to release RNA molecules from the gel and recapture them on the array surface (Extended Data Fig. 1a–d). Reverse transcription and library preparation was then performed using a modified version of the standard Visium protocol, which enhanced RNA capture efficiency with longer capture probes and thereby the final library quality (see Methods, Extended Data Fig. 1e–g).

We first performed Ex-ST on the mouse olfactory bulb (MOB), in which neurons are organized in spatially distinct laminated zones with well-defined molecular signatures[9,10]. With matched sequencing saturation (Extended Data Table. 1), Ex-ST captured more unique molecular identifiers (UMIs) per gene from the same tissue area compared to the standard Visium protocol (median: Ex-ST = 29.5 ± 2.5, Visium = 14 ± 2, n=2; Fig. 1b), and showed excellent reproducibility between replicates (Extended Data Fig. 2a). As expected, the number of unique molecules and genes detected per spot was lower using Ex-ST, but after normalizing the tissue area covering each spot, Ex-ST captured more UMIs (median: Ex-ST = 682.5 ± 16, Visium = 503 ± 29, n=2, in areas of 20 μm in diameter; Extended Data Fig. 1g) and unique genes (median: Ex-ST = 430.5 ± 8.5, Visium = 230 ± 21, n=2; Fig. 1c). These observations suggest that Ex-ST achieves higher coverage of transcripts.

To examine potential bias that may be introduced by the Ex-ST protocol, we first compared gene expression measured by Ex-ST, standard Visium, bulk RNAseq[11], and Slide-seq[12], which showed broad agreement between methods (Extended Data Fig. 2b–d). This is further supported by similar RNA biotype composition, 3’ bias in gene body coverage, and size distribution of captured transcripts comparing Ex-ST and standard Visium (Extended Data Fig. 2e–g). We also noticed that Ex-ST captured more intronic reads, potentially due to the protocol modifications and protein digestion step that better exposed the nuclear RNA (Extended Data Fig. 2h).

The spatial distribution of region-specific marker genes, including *Sox11* for subependymal zone (SEZ), *Nrgn* for granular layer (GCL), *Cdhr1* for mitral (M) and tufted (T) cell layers, *Nrsn1* for glomerular layer (GL), and *Ptn* for olfactory nerve layer (ONL)[9], showed expected layered patterns (Fig. 1d, Extended Data Fig. 3a)[10], and indeed had higher UMI counts compared to the standard Visium protocol (Extended Data Fig. 3b). By clustering the

Ex-ST data, we identified 6 clusters, each corresponding to a morphological layer of MOB, annotated based on their marker genes and spatial locations (Fig. 1e, Extended Data Fig. 3c–e). In particular, SEZ and M/T clusters covered only 1–2 lines of spots, consistent with the width (< 50 μm) of these layers (Fig. 1f).

We next determined whether tissue expansion reduced the number of cells occupying each spot. We applied stereoscope, a deconvolution algorithm to infer cell type composition of each spot using single-cell transcriptomes[13]. We observed that Ex-ST data contained more spots with single dominant cell type, in comparison to both the standard and modified Visium protocols (Extended Data Fig. 4). For example, SEZ and M/T regions had 16 and 96 spots, respectively, where a single cell type occupancy was over 50% with highest values reaching ~80%. In contrast, standard Visium data had no spots in SEZ and only 2 in the M/T region, with dominating cell type occupancy barely over 50%, suggesting that Ex-ST can better separate cell types in space (Fig. 1g).

Encouraged by the enhanced resolution of Ex-ST, we examined the glomeruli in olfactory bulbs, whose sizes range between 50 to 120 μm in diameter. Consequently, resolving gene expression within individual glomeruli using standard Visium is challenging. In contrast, Ex-ST allowed us to map olfactory receptors directly onto single glomeruli (Fig. 1h), consistent with previous findings that olfactory sensory neurons projecting their axons into a common glomerulus should express the same type of olfactory receptor (Olfr)[14,15]. This result demonstrates the potential of Ex-ST to reveal tissue organization at a finer scale.

Applying Ex-ST on mouse hippocampus, we identified 11 clusters corresponding to different anatomical regions, expressing known marker genes (Fig. 2a, Extended Data Fig. 5a–c), while the expression levels are consistent between Ex-ST and standard Visium (Extended Data Fig. 5d–h). Stereoscope analysis showed that most spots in the cornu ammonis (CA) and dentate gyrus (DG) regions had >80% of occupancy by a single cell type whereas the standard Visium data rarely had spots with cell type occupancy over 50% (Fig. 2b, Extended Data Fig. 6a). Overall, Ex-ST shifted the cell type composition per spot towards single cell type occupancy throughout the hippocampus (Fig. 2c).

Notably, by expanding the tissue, we resolved subclasses of oligodendrocytes in alveus, a dense layer of myelinated axonal fibers covering the ventricular parts of the hippocampus. Consistent with *in situ* hybridization (ISH), oligodendrocyte markers, such as *Tspan2*, were distributed sporadically within this layer in our Ex-ST data, whereas their expression in the standard Visium data was more continuous and diffusive (Fig. 2d, Extended Data Fig. 6b). Deconvolving the expression of individual spots using stereoscope revealed the distinct patterns of several oligodendrocyte subtypes in the Ex-ST data, including myelin forming oligodendrocyte (MFOL) and mature oligodendrocyte (MOLG)[16], which were mixed in the standard Visium data (Fig. 2e, Extended Data Fig. 6c). This observation suggests that Ex-ST improves the capacity of distinguishing spatially-mixed sub-cell types that are only subtly different.

Lastly, we demonstrated that Ex-ST could measure subcellular distribution of transcripts. While most neurons have more transcripts in somata, CA1 neurons actively transport

specific transcripts to dendrites[17]. Indeed, the total number of UMIs dropped from the somata into stratum radiatum in a distance matching the expected size of somata (~125 μm) (Fig. 2f), suggesting that the lateral diffusion of transcripts during RNA capture is negligible. With higher spatial resolution, Ex-ST was able to resolve differentially located transcripts in somata and dendrites, including dendrite-enriched genes such as *Psd* and *Git1* (Fig. 2g, h). Through differential gene expression analysis and after removing glial transcripts, Ex-ST identified ~500 dendrite-enriched genes that were unresolvable with the standard Visium protocol, all of which overlapped with at least one of the three previous studies using orthogonal methods to identify dendritic transcripts in CA neurons (Fig. 2i, Extended Data Fig. 6d, Extended Data Table. 2)[18–20].

In summary, Ex-ST overcomes the density limitation of spatially barcoded capture arrays by expanding polyelectrolyte gels to which RNA molecules are anchored. The advances made in this study are in two major aspects. First, enlarged biological structures cover more capture spots, which pushes the spatial resolution of the Visium array from 55 to 20 μm. Second, optimizing RNA capture is crucial for Ex-ST, as it enables the detection of more transcripts from fewer cells per spot. Although the gel embedding and expansion steps take additional processing time (~3 d) compared to the standard Visium protocol, Ex-ST does not require specialized equipment needed in imaging based *in situ* sequencing methods (see Supplementary Discussion for more comparison between Ex-ST and other high resolution ST techniques). Finally, our approach is orthogonal to other method development efforts in the field that have primarily focused on shrinking the capture spot size[2,3,18,21], thereby, can be potentially integrated with other techniques to enhance their performance as well.

Methods

Animals

Adult male CD1 mice (3–6 months old, Charles River) were used for the Ex-ST experiments. Animal procedures were approved by the Stanford University Animal Care and Use Committee and were in accordance with NIH guidelines. Animals were maintained with 12-hour light-dark cycle, with ambient temperature between 71–74 °F, humidity between 20–45 %, and provided with food and water *ad libitum*. Mouse olfactory bulb samples for standard Visium experiment were commercially purchased from Adlego Biomedical, which operates under ethical permission nr. 17114–2020.

Tissue preparation

Animals were euthanized by CO_2 followed by cervical dislocation. Brain tissue was quickly dissected and embedded in O.C.T. (Tissue tek, cat# 981385). The tissue block was snap-frozen using liquid nitrogen vapor until the O.C.T. block was hardened and stored in −80 °C until use. Tissues were cryosectioned to 15 μm thickness on a Leica cryostat and placed onto charged glass slides (VWR, cat# 75799).

Visium slides for Ex-ST

Ex-ST used multimodal spatial arrays. Each capture area has dimensions of 6.5 × 6.5 mm, containing 5,000 spots each with a diameter of 55 um. Surface capture probes include

spatial barcodes, UMIs, and 50 TVN sequence to allow for polyA mediated capture of RNA molecules.

Expansion

All steps prior to RT were performed on charged glass slides (VWR). This eliminates the uneasy task of placing a tissue section into the Visium capture area, which can result in a failed positioning or tissue folding requiring a slide reset. Sections were fixed with acetone for 1 h at −20 °C, followed by incubation in the hybridization buffer, containing 1 μM anchor probe[23] (a 15-nt sequence of alternating dT and thymidine-locked nucleic acid (dT+) with a 5′-acrydite modification, Integrated DNA Technologies), 2× SSC, 30% [v/v] formamide (Millipore Sigma, cat# 11814320001), 0.1% [w/v] yeast tRNA (Calbiochem, cat #55714), 1% [v/v] RNase inhibitor (Progma, cat# N2615), and 10% [w/v] dextran sulfate (Sigma, cat# D8906), at 37 °C under saturation humidity for 40 h. After anchor probe hybridization, sections were washed three times with 1× SSC.

Expansion protocol followed a sequence of gelation, proteinase K digestion, and expansion, as previously described[24]. Briefly, samples were washed three times in PBS, then incubated in the monomer solution (1× PBS, 2 M NaCl, 8.625% [w/w] sodium acrylate, 2.5% [w/w] acrylamide, 0.15% [w/w] N,N′-methylenebisacrylamide) for 45 min at 4°C. Gelation was initiated by adding 0.2% [w/v] ammonium persulfate (ThermoFisher Scientific, cat# 17874), 0.01% [w/w] 4-hydroxy-2,2,6,6-tetramethylpiperidin-1-oxyl (4-hydroxy-TEMPO, Sigma-Aldrich, cat# 176141), 0.2% [w/w] tetramethylethylenediamine (ThermoFisher Scientific, cat# 17919). The gelation step was performed at 37°C for 1–2 h.

After gelation, samples were gently removed from the chamber and digested overnight at 37°C in 8 U mL^{-1} proteinase K (NEB, cat# P8107) in digestion buffer (1× TAE buffer, 0.5% Triton X-100, 0.8 M guanidine HCl). Gels were then removed from the digestion buffer and placed in 0.1× SSC to expand. 0.1× SSC was exchanged every 15 min for 3–5 times until the gel size plateaued. To stain nuclei, expanded samples were incubated with 100 μM DAPI in 0.1× SSC for 30 min. Both bright field and DAPI images of expanded samples were taken after the gel was placed on top of the Visium array and prior to RNA release and reverse transcription (RT).

Ex-ST library preparation

First, to determine the optimal temperature for RNA release from the gel, several temperatures were tested. We analyzed the released RNAs using bioanalyzer (Agilent 2100) to measure concentration and length distribution (Extended Data Fig. 1a). We observed that RNA molecules were released from the gel with high integrity as long as temperature exceeded 41 °C (Extended Data Fig. 1b–d). We did not notice significant differences in the released RNA concentration between 41 °C and 45 °C (Extended Data Fig. 1d) and therefore chose to perform the experiment at 45 °C for 30 min to ensure that RNA molecules are fully released from the gel and to prevent re-hybridization with anchor probes.

RT was modified from the standard protocol to be conducted at 42 °C for 60 min followed by 53 °C for 45 min using the Visium Spatial Gene Expression reagents (10x Genomics). This extended time of RT was chosen to enhance the reaction efficiency. After RT, the

second strand synthesis was performed according to the 10x Genomics Visium Spatial Gene Expression protocol, followed by qPCR to determine the number of amplification cycles. An extra PCR cycle was added in the amplification step, in addition to the recommended number of cycles in the Visium Gene Expression protocol. A higher concentration of SPRIselect beads (0.8×, instead of 0.6× in the standard Visium protocol) was used in the post-amplification cleanup step to retain more fragments. The rest of the library preparation was carried out according to the 10x Genomics Visium Spatial Gene Expression protocol (User Guide CG000239_RevF). Finished libraries were sequenced on a NextSeq 2000 platform (Illumina).

To quantify how these protocol modifications and longer surface probes may affect RNA capture efficiency, we applied the modified protocols (without expansion) on MOB sections of 15 μm in thickness, matching the tissue sections used for the Ex-ST experiments. This experiment generated libraries with high complexity, leading to low sequencing saturation (~60%) even with high numbers of sequencing reads per spot (Extended Data Table. 1). For fair comparison, we downsampled the Ex-ST and standard Visium datasets using *Seqtk* (version 1.3) package in order to match the sequencing saturation across experiments. We found that the modified protocol detected higher UMIs (mean: standard Visium = 38.5 ± 5.5, modified Visium = 538 ± 13, n=2) per gene and number of genes (mean: standard Visium = 163.5 ± 14.5, modified Visium = 1270.5 ± 5.5, n=2) per tissue area (Extended Data Fig. 1e–g). Since incomplete poly-dT probe hybridization, tissue digestion and gel expansion may result in transcript loss, these modifications are crucial to implement Ex-ST, as they allow the detection of more transcripts from fewer cells compared to the standard Visium protocol (Extended Data Fig. 1e–g).

Image acquisition and processing

Bright field and DAPI images of expanded samples were taken on a Zeiss Axio Observer Z1 inverted microscope equipped with an Axiocam 503M camera and a 5×/0.25 objective using Zen Pro 2012 software. The imaging time was minimized to prevent gel from drying and shrinking. Bright field image of the array frame and gel position within each capture area was aligned with the corresponding DAPI image. Manual selection of spots under the tissue was done using Loupe Browser (v 4.0.0, 10x Genomics).

Standard Visium library preparation of MOB

The fresh-frozen MOB sample was cryo-sectioned at 10 μm thickness, placed onto Visium glass slides and stored at −80 °C prior processing. The spatial gene expression libraries were prepared according to the manufacturer's protocol (Visium Spatial Gene Expression, User Guide CG000239_RevC). Finished libraries were sequenced on a NextSeq 2000 platform (Illumina).

Data processing

The MOB data generated by the standard Visium protocol were processed by space ranger software (version 1.0.0, 10x Genomics). All Ex-ST data were processed by space ranger software (version 1.3.0 adapted to work with custom barcode list, 10x Genomics). Reads were aligned to the pre-built mouse reference genome (mm10, 10x Genomics). Processed

output files for the standard Visium data of the coronal mouse brain section containing the hippocampus region were downloaded from 10x Genomics website.

Data analysis

Analysis of data generated by both Ex-ST and standard Visium was performed in Python (version 3.7.12) and R (version 4.0.5). Spots with fewer than 100 genes detected (UMI > 1) were excluded from the analysis. For spatial gene expression plotting and differential gene expression analysis, expression at each spot was normalized using Scanpy (version 1.8.2) to the same total count. Dimensional reduction and clustering were performed using the Self-Assembling Manifolds (SAM) algorithm (version 0.8.9)[25] with default parameters. Spot deconvolution analysis was performed using stereoscope[13]. The mouse brain single-cell RNAseq data used for deconvolution was the “Adolescent mouse brain” dataset obtained from http://mousebrain.org/. Spatial plots for cell type mapping were produced in R (version 4.0.5), using the Seurat (version 4.1.1) and *STUtility* (version 0.1.0) R packages. CA1 soma and dendrite regions used for differential gene expression analysis were selected manually based on the DAPI images.

To examine whether sequencing saturation affects spot devolution analysis and dendritic gene discovery, we downsampled the Ex-ST data using *Seqtk* (version 1.3) package to match lower sequencing saturation of the 10x Genomics mouse hippocampus dataset. After downsampling, spots in the major hippocampal regions, including CA and DG, still had single cell type occupancy over 80% (Extended Data Fig. 6a). We were still able to resolve distinct patterns of oligodendrocyte subtypes (Extended Data Fig. 6c) and identify over 90% of dendrite-enriched genes, which were undetected using the standard Visium protocol (Extended Data Table. 2).

Statistics and Reproducibility

P-values were calculated via Mann-Whitney-Wilcoxon test or Welch’s t-test as indicated using sciPy library (version 1.9.1) with default parameters. Gene expression profiles along the soma-dendrite axis were generated by averaging the expression of spots at the same distance from the soma region. All spatial profiles of gene expression, cluster annotation, and cell type occupancy shown in this study were representative images from two independent replicates.

Extended Data

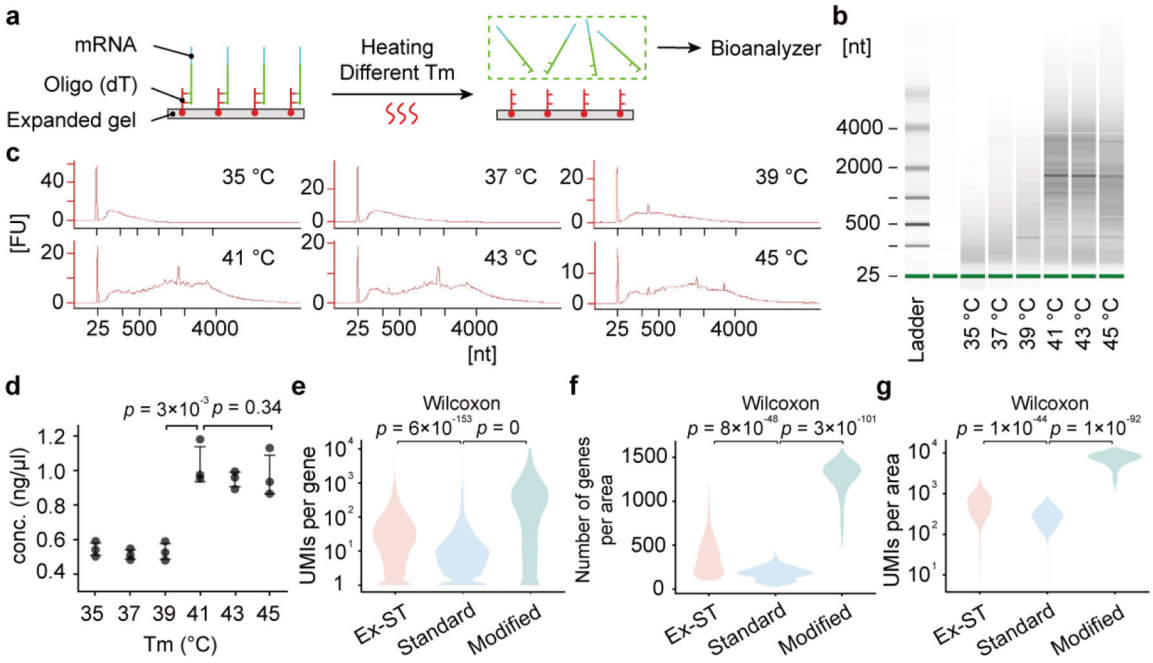

Extended Data Fig. 1: RNA release and capture.

a, The workflow to identify the optimal release temperature. Gel with anchored transcripts was heated for 30 min at different temperatures to release RNA molecules, which were collected and quantified on a Bioanalyzer. **b,** Representative bioanalyzer gel image from three replicates, showing RNA released from the gel at different incubation temperatures. **c,** Representative bioanalyzer traces showing the released RNA. Only weak rRNA peaks are expected as the RNA anchoring is mediated by polyA. **d**, Released RNA concentrations at different incubation temperatures measured from three biological replicates. Error bars: mean ± standard derivation (SD). Increasing temperature from 39 °C to 41 °C significantly increased RNA concentrations, whereas no significant difference was observed above 41 °C. *P* values: two-sided Welch's t-test. **e,** Violin plot showing the number of UMIs per gene detected by Ex-ST and Visium using standard and modified protocols. **f-g,** Comparisons of number of genes (**f**) and UMIs (**g**) per tissue area (20 by 20 µm) measured by Ex-ST and Visium using the standard and modified protocols, calculated by normalizing the number of genes and UMIs per spot by the tissue area covering each spot. Ex-ST and standard Visium data in **e-g** were downsampled to match sequencing saturation (Extended Data Table. 1). *P* values: two-sided, two-sample Mann-Whitney-Wilcoxon tests.

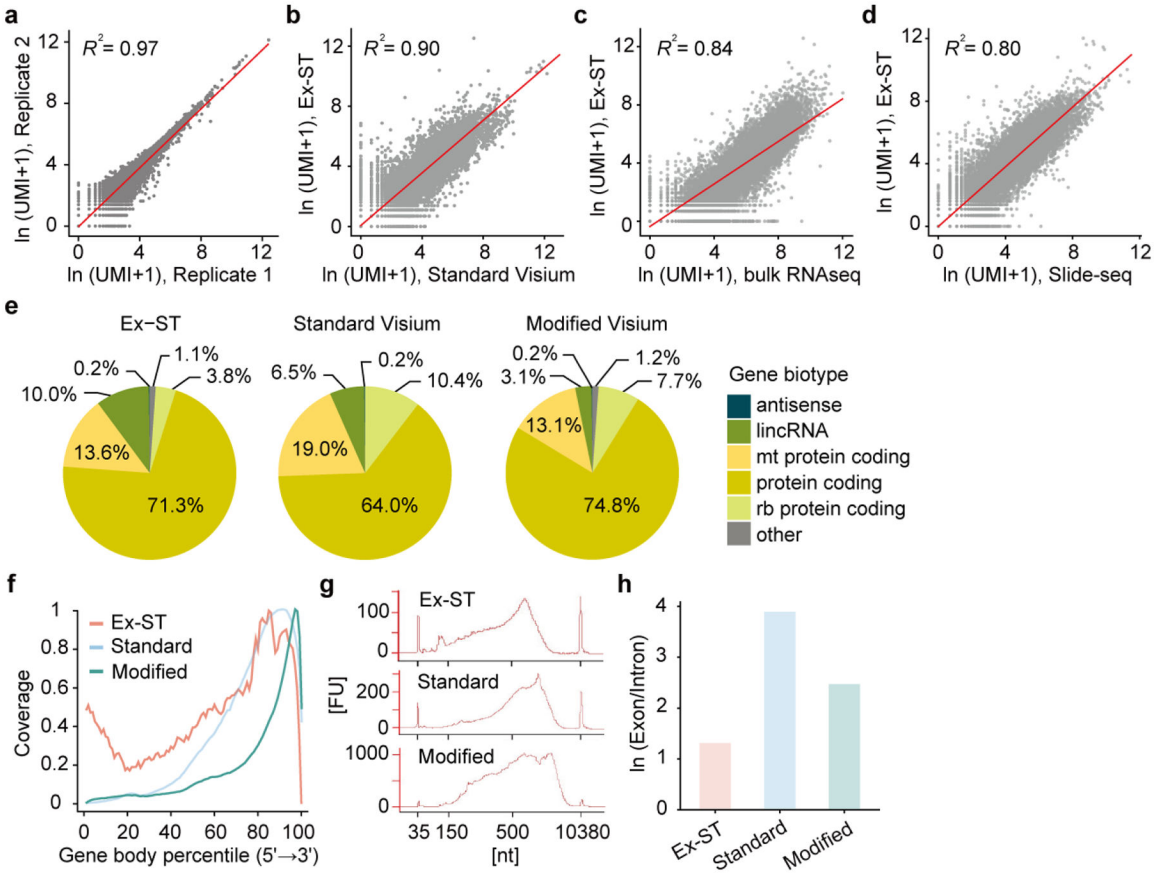

Extended Data Fig. 2: Ex-ST captures RNA with limited biases.

a, Comparison of the number of UMIs per gene between two Ex-ST MOB replicates. **b-d,** Comparisons of the number of UMIs per gene detected in the Ex-ST and standard Visium MOB datasets (**b**), in the Ex-ST and bulk RNAseq MOB datasets (**c**) and in the Ex-ST and Slide-seq hippocampus datasets (**d**). Red lines: least squares linear fit. **e,** Pie charts showing RNA biotypes captured by Ex-ST and Visium using standard and modified protocols. Proportions are quantified by the total UMI counts of each biotype. **f,** Gene body coverage for the Ex-ST and standard/modified Visium data. **g,** Bioanalyzer traces of cDNA before the fragmentation step for the Ex-ST and standard/modified Visium protocols. **h**, Ratio of exonic and intronic reads in the Ex-ST and standard/modified Visium data.

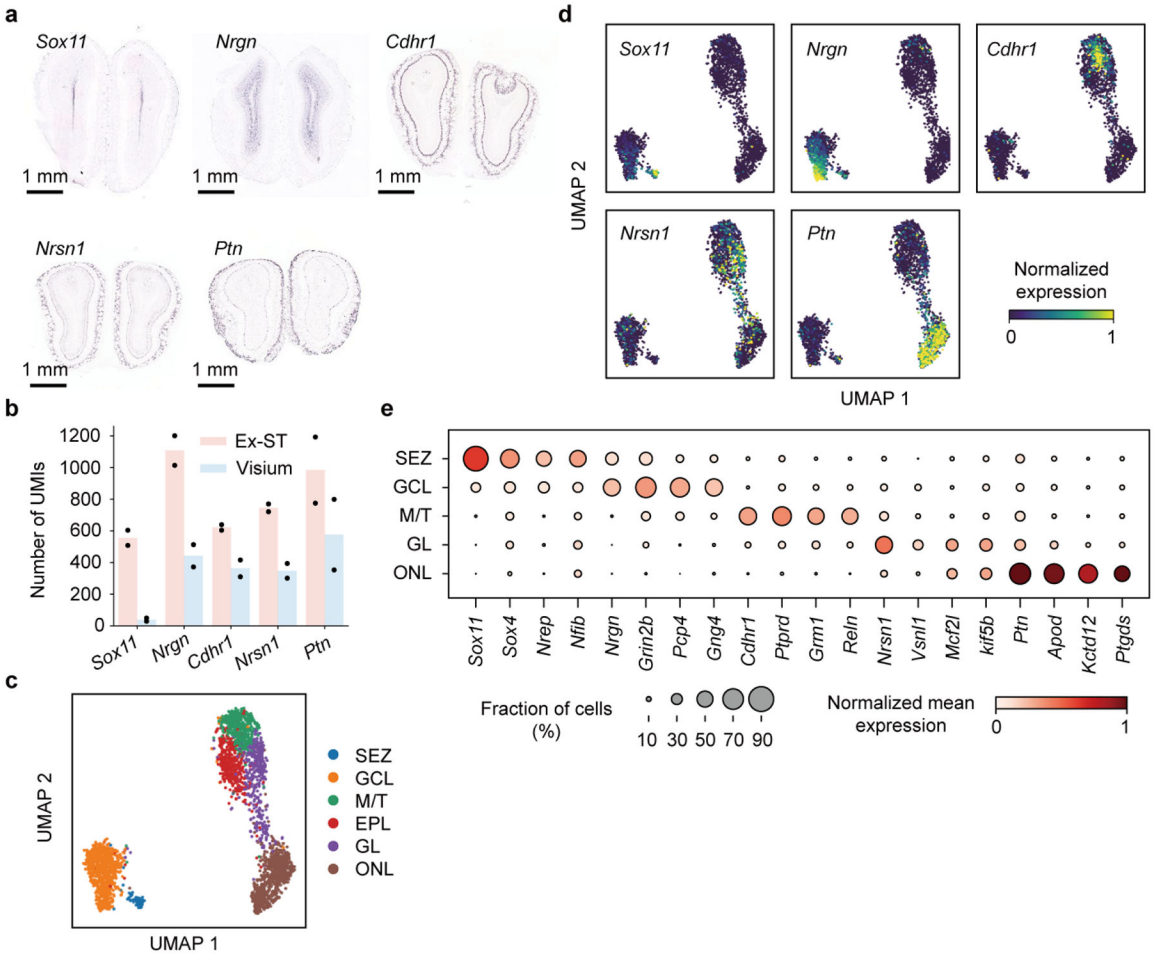

Extended Data Fig. 3: Annotation of spatial clusters of the MOB Ex-ST data.

a, The expression of region-specific marker genes detected by ISH, obtained from Allen Brain Atlas [10]. **b,** Comparison of number of UMIs of select region-specific marker genes measured by Ex-ST and standard Visium from matched tissue areas. Bar charts: mean of two replicates. **c,** UMAP showing Ex-ST MOB clusters identified by unsupervised clustering, colored by cluster annotation. **d,** Marker gene expression overlaid on the UMAP visualization. **e,** Dot plot showing top marker genes for each cluster.

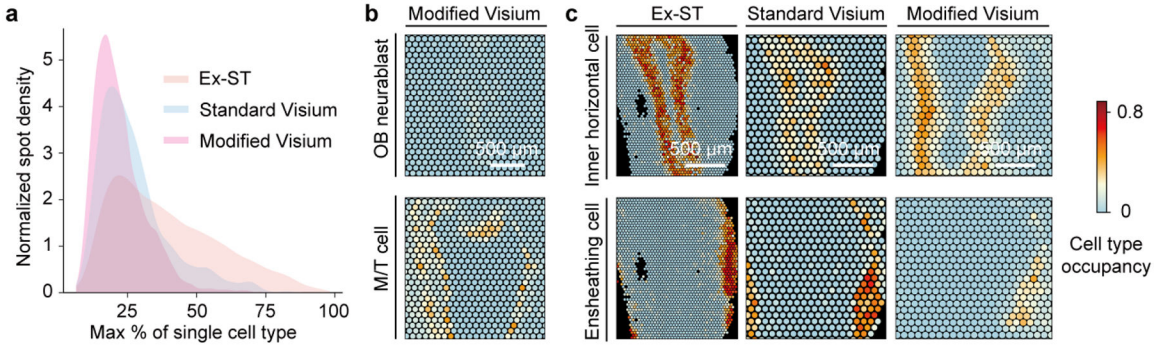

Extended Data Fig. 4: Cell type compositions of spots in the MOB datasets.

a, Density plot showing the distribution of dominating cell type occupancy at each spot for Ex-ST and Visium using standard and modified protocols. **b**, Cell type occupancy of each spot in the modified Visium data visualized for two cell types, OB neuroblasts and M/T cells. **c,** Comparison of cell type composition at individual spots in the Ex-ST, standard Visium, and modified Visium datasets visualized for two cell types, inner horizontal cells located in GCL and ensheathing cells in ONL.

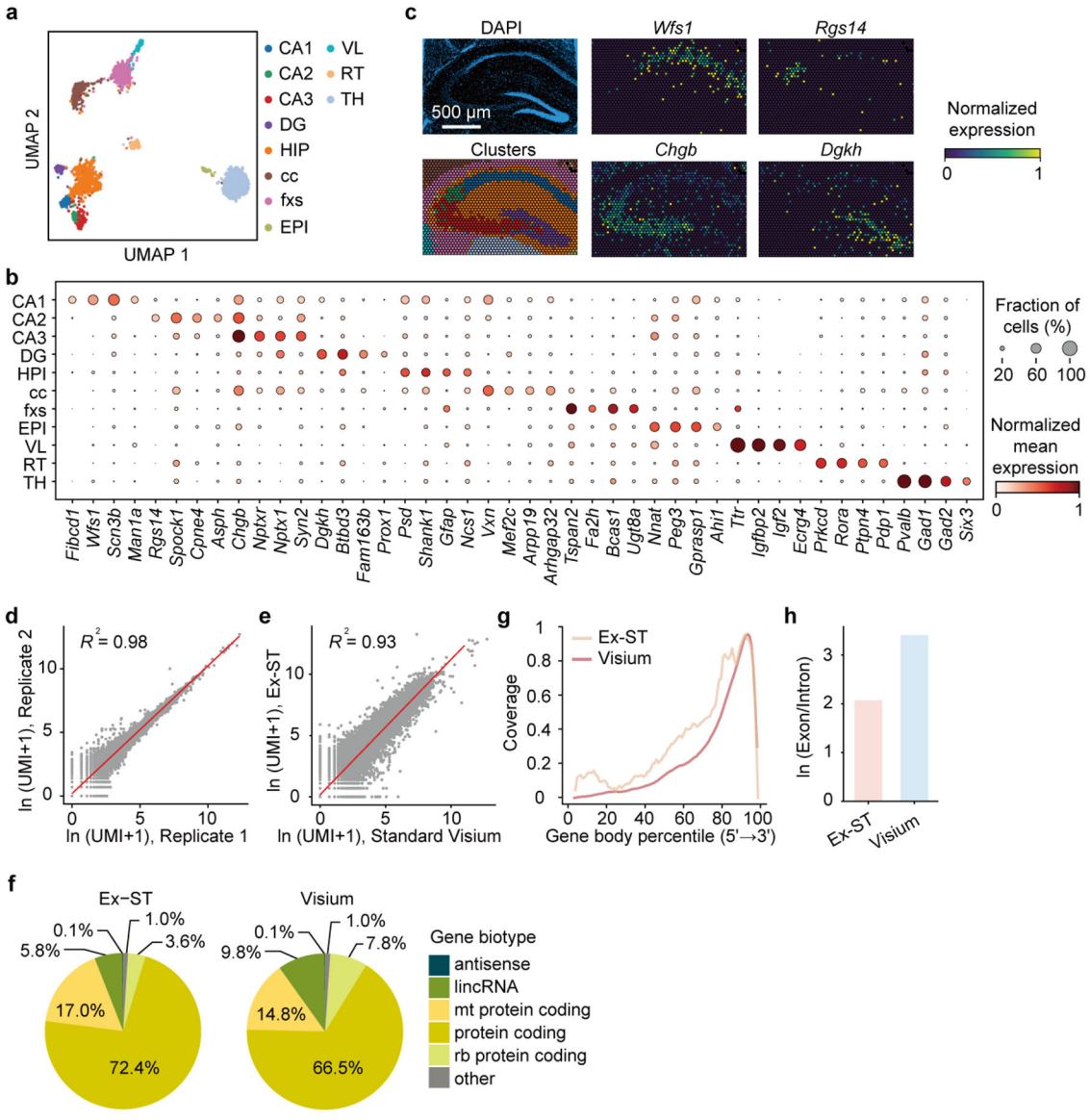

Extended Data Fig. 5: Characterization of the Ex-ST mouse hippocampus data.

a, UMAP showing the annotated clusters identified by unsupervised clustering of the Ex-ST hippocampus data. **b,** Dot plot showing the top marker genes of each cluster. **c,** Spatial gene expression of region-specific marker genes measured by Ex-ST, i.e., *Wfs* for CA1, *Rgs14* for CA2, *Chgb* for CA3, *Dgkh* for DG. **d,** Comparison of the number UMIs per gene between the Ex-ST replicates. **e,** Comparison of the number of UMIs per gene in the Ex-ST and

standard Visium datasets. **f,** Pie charts showing RNA biotype composition in the Ex-ST and standard Visium data. Proportions are quantified by the UMI counts of each biotype. **g,** Gene body coverage of the Ex-ST and standard Visium data. **h**, Ratio of exonic and intronic reads in the Ex-ST and standard Visium datasets.

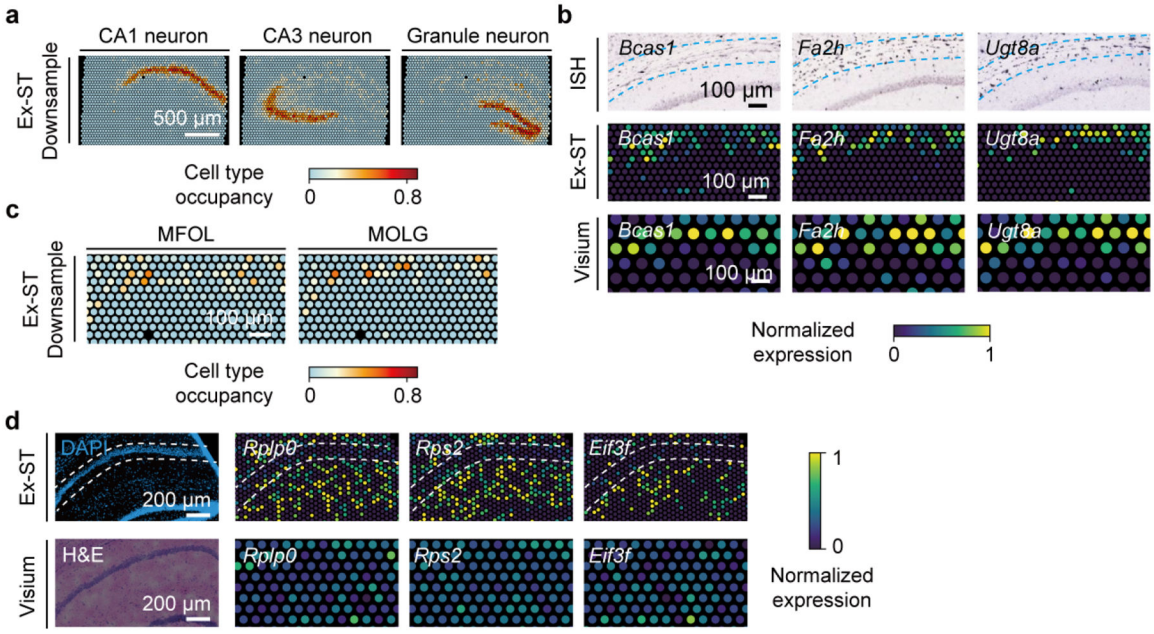

Extended Data Fig. 6: Ex-ST hippocampal data has higher spatial resolution compared to standard Visium.

a, Cell type composition of individual spots in the Ex-ST data downsampled to match the sequencing saturation of the 10x Genomics dataset. Three major neuronal cell types are shown. Note that the patterns are almost identical to Fig. 2b, suggesting that cell type devolution is mostly insensitive to sequencing depth in the regime of 60–90% saturation. **b,** Comparison of ISH (top), obtained from Allen Brain Atlas [10], normalized spatial expression of oligodendrocyte marker genes detected by Ex-ST (middle) and standard Visium (bottom). **c,** Cell type composition of individual spots in Ex-ST downsampled to match the sequencing saturation of the 10x Genomics data. Oligodendrocyte subclasses are shown, with patterns identical to Fig. 2e. **d,** Comparison of normalized spatial distribution of lowly-expressed dendrite-enriched transcripts between Ex-ST and standard Visium. Note the lack of pattern in the standard Visium data.

Extended Data Table. 1:
Sample information obtained from space ranger software (10x Genomics) output.

Visium MOB datasets obtained using the standard/modified protocols were collected on tissue sections containing two bulbs. Both bulbs are combined to compare with the expanded MOB data with two replicates each containing one bulb. Downsampled Ex-ST and standard Visium MOB data have sequencing saturation matching with the data generated using the modified protocol. Hippocampus data includes matched tissue areas from coronal sections of the mouse brain in the hippocampal region. Downsampled Ex-ST hippocampus data have sequencing saturation matching with the 10x Genomics hippocampus data. With matched sequencing saturation, the Ex-ST data always contain fewer reads per spot compared to the Visium datasets. This is expected as each spot in the Ex-ST data corresponds to fewer cells and therefore should have lower library complexity.

Sample name	Number of spots under tissue	Sequencing saturation	Mean reads per spot
Ex-ST_MOB_replicate_1	2 774	93.50%	33 591
Ex-ST_MOB_replicate_2	2 331	94.10%	35 598
Standard_Visium_MOB	1 301	91.70%	86 429
Ex-ST_MOB_replicate_1_downsampled	2 774	61.60%	3 605
Ex-ST_MOB_replicate_2_downsampled	2 331	61.80%	3 432
Standard_Visium_MOB_downsampled	1 301	57.20%	7 663
Modified_Visium_MOB_replicate_1	1 448	60.30%	249 532
Modified_Visium_MOB_replicate_2	1 490	57.40%	183 162
Ex-ST_Hippocampus_replicate_1	3 049	88.80%	25 660
Ex-ST_Hippocampus_replicate_2	3 191	89.00%	33 928
Standard Visium Hippocampus (10x Genomics dataset)	2 698	61.90%	115 740
Ex-ST_Hippocampus_replicate_1_downsampled	3 049	60.30%	4 395
Ex-ST_Hippocampus_replicate_2_downsampled	3 191	59.70%	5 659

Extended Data Table. 2:
Dendrite-enriched transcripts.

Dendrite-enriched transcripts detected by Ex-ST but unresolvable using the standard Visium protocol are listed. Also provided are the previous measurements [18–20] that support the dendritic expression of these transcripts and whether these transcripts are detected in the downsampled Ex-ST data.

Gene name	Detected by Ex-ST?	Detected by ST?	Detected by downsampled Ex-ST?	Detected by Joshua, et al.?	Detected by Tushev, et al.?	Detected by Slide_seq V2?
1700017B05Rik	Y	N	Y	Y		
2700081O15Rik	Y	N	Y	Y		
4930481A15Rik	Y	N	Y	Y		
Aaas	Y	N	Y	Y		

Gene name	Detected by Ex-ST?	Detected by ST?	Detected by downsampled Ex-ST?	Detected by Joshua, et al.?	Detected by Tushev, et al.?	Detected by Slide_seq V2?
Abat	Y	N	Y			Y
Abcd1	Y	N	Y	Y		
Abcd2	Y	N	Y		Y	Y
Abhd4	Y	N	Y	Y		
Abl1	Y	N	Y	Y		
Acadm	Y	N	Y	Y		
Acat3	Y	N	Y	Y		
Acsf2	Y	N	Y		Y	
Acsl6	Y	N	Y	Y		Y
Adap1	Y	N	Y		Y	
Adarb1	Y	N	Y		Y	
Adarb2	Y	N	Y	Y		Y
Adcy1	Y	N	Y	Y		
Adcy5	Y	N	Y			Y
Adcyap1r1	Y	N	Y	Y	Y	
Afg3l1	Y	N	Y	Y		
Agap1	Y	N				Y
Agl	Y	N	Y	Y		
AI506816	Y	N	Y	Y		
Akt2	Y	N	Y	Y		
Aldh6a1	Y	N		Y		
Ankrd13a	Y	N	Y	Y		
Ankrd26	Y	N	Y	Y		
Ankrd40	Y	N		Y		
Anp32e	Y	N	Y	Y		
Ap3s2	Y	N	Y			Y
Apba1	Y	N	Y	Y		
Apod	Y	N	Y	Y		
Arhgap11a	Y	N			Y	
Arhgap30	Y	N	Y		Y	
Arhgap33	Y	N	Y	Y		
Arid3a	Y	N	Y	Y		
Arl3	Y	N	Y		Y	
Arl6ip6	Y	N	Y	Y		
Armcx6	Y	N	Y	Y		
Arnt2	Y	N	Y	Y	Y	
Arpc1b	Y	N	Y	Y		
Arpp21	Y	N	Y	Y		
Arrdc3	Y	N	Y	Y		
Arxes2	Y	N	Y	Y		

Gene name	Detected by Ex-ST?	Detected by ST?	Detected by downsampled Ex-ST?	Detected by Joshua, et al.?	Detected by Tushev, et al.?	Detected by Slide_seq V2?
Asrgl1	Y	N	Y			Y
Atp1a2	Y	N	Y	Y		Y
Atr	Y	N	Y		Y	
Baalc	Y	N	Y			Y
Bach2	Y	N	Y	Y		
Bak1	Y	N	Y	Y		
Bard1	Y	N	Y	Y		
Baz1a	Y	N	Y		Y	
BC030867	Y	N	Y	Y		
BC035044	Y	N	Y	Y		
Bcr	Y	N		Y		
Begain	Y	N	Y	Y		
Bloc1s1	Y	N	Y	Y		
Bola2	Y	N	Y	Y		
Brix1	Y	N	Y	Y		
Brpf3	Y	N	Y	Y		
Btbd3	Y	N	Y			Y
C030006K11Rik	Y	N	Y	Y		
Cbfa2t3	Y	N	Y			Y
Ccdc88a	Y	N	Y	Y		
Cd63	Y	N		Y		
Cd79b	Y	N			Y	
Cdc42ep1	Y	N	Y	Y		
Cdc42ep4	Y	N	Y	Y		
Cdk16	Y	N	Y	Y		Y
Cdk2ap1	Y	N	Y	Y		
Cep250	Y	N	Y	Y		
Cfh	Y	N	Y	Y		
Chaf1a	Y	N	Y	Y		
Chaf1b	Y	N			Y	
Chd3	Y	N	Y	Y		
Chmp1a	Y	N	Y	Y		
Chrna4	Y	N	Y	Y		Y
Cib2	Y	N	Y	Y		Y
Cic	Y	N	Y	Y		
Cit	Y	N	Y	Y		Y
Clic4	Y	N	Y	Y		
Clmn	Y	N	Y			Y
Clu	Y	N	Y			Y
Cnp	Y	N	Y	Y		

Gene name	Detected by Ex-ST?	Detected by ST?	Detected by downsampled Ex-ST?	Detected by Joshua, et al.?	Detected by Tushev, et al.?	Detected by Slide_seq V2?
Cnpy3	Y	N	Y	Y		
Cnr1	Y	N	Y			Y
Cntfr	Y	N	Y	Y		
Coa7	Y	N	Y	Y		
Coil	Y	N	Y	Y		
Cox15	Y	N	Y	Y		
Cox7a2l	Y	N	Y	Y		
Cplx2	Y	N	Y			Y
Cpne3	Y	N	Y	Y		
Crip1	Y	N	Y	Y		
Crot	Y	N		Y		
Crtc1	Y	N	Y	Y		
Csdc2	Y	N				Y
Csrnp2	Y	N	Y	Y		
Ctnnbip1	Y	N	Y			Y
Ctnnd2	Y	N	Y	Y	Y	Y
Ctsz	Y	N	Y	Y		
Cul4b	Y	N	Y	Y		
Cuta	Y	N	Y	Y		
Cux1	Y	N		Y		
Cyb5d1	Y	N	Y	Y		
D8Ertd738e	Y	N	Y	Y		Y
Dab2ip	Y	N	Y	Y		
Dad1	Y	N	Y	Y		
Dbndd1	Y	N	Y	Y		
Dbnl	Y	N	Y		Y	
Ddit4l	Y	N	Y	Y		
Dennd2a	Y	N	Y	Y		
Dgkeos	Y	N	Y	Y		
Dio2	Y	N				Y
Dlg2	Y	N	Y	Y		Y
Dlgap2	Y	N	Y	Y		
Dlgap3	Y	N	Y	Y		
Dmwd	Y	N	Y	Y		
Dnajc19	Y	N	Y	Y		
Dnajc2	Y	N	Y	Y		
Dnajc27	Y	N	Y	Y		
Dnm2	Y	N	Y	Y		
Dok6	Y	N	Y			Y
Dolpp1	Y	N	Y	Y		

Gene name	Detected by Ex-ST?	Detected by ST?	Detected by downsampled Ex-ST?	Detected by Joshua, et al.?	Detected by Tushev, et al.?	Detected by Slide_seq V2?
Drap1	Y	N	Y	Y		Y
Dtl	Y	N	Y		Y	
Dtx3l	Y	N	Y	Y		
Dusp15	Y	N	Y			Y
Dusp16	Y	N	Y	Y		
Dyrk1b	Y	N	Y	Y		
Dzip1	Y	N	Y	Y		
E130114P18Rik	Y	N	Y	Y		
E2f1	Y	N	Y	Y		
E2f2	Y	N			Y	
Edem1	Y	N	Y	Y		
Eef1b2	Y	N	Y	Y		
Eif2d	Y	N	Y	Y		
Eif3f	Y	N	Y	Y		
Eif3h	Y	N	Y	Y		
Eif3j1	Y	N	Y	Y		
Eif4ebp2	Y	N	Y	Y		
Enho	Y	N	Y	Y		
Enpp2	Y	N	Y	Y		
Epas1	Y	N	Y	Y		Y
Epb41l1	Y	N	Y			Y
Epn1	Y	N	Y	Y	Y	
Eps8	Y	N		Y		
Evi5l	Y	N	Y	Y		
Ezh2	Y	N	Y	Y		
Ezr	Y	N	Y	Y		
Fam102a	Y	N	Y	Y		
Fam111a	Y	N	Y	Y		
Fam149b	Y	N	Y	Y		
Fam163a	Y	N	Y		Y	Y
Fam177a	Y	N	Y		Y	
Fam184a	Y	N	Y	Y		
Fasn	Y	N	Y		Y	
Fat1	Y	N	Y	Y		
Fbl	Y	N	Y	Y		
Fbxo41	Y	N	Y	Y		Y
Fgd2	Y	N	Y	Y		
Fgf1	Y	N	Y	Y		
Fgf11	Y	N	Y	Y		
Fgf13	Y	N	Y	Y		Y

Gene name	Detected by Ex-ST?	Detected by ST?	Detected by downsampled Ex-ST?	Detected by Joshua, et al.?	Detected by Tushev, et al.?	Detected by Slide_seq V2?
Fkbp2	Y	N	Y	Y	Y	
Fmn1	Y	N	Y	Y		
Fmn2	Y	N	Y	Y		
Fosb	Y	N	Y			Y
Foxo3	Y	N	Y	Y		
Ftl1	Y	N	Y	Y		
Fxyd1	Y	N	Y	Y		Y
G6pc3	Y	N	Y	Y		
Gabrg1	Y	N	Y	Y	Y	
Gad2	Y	N	Y	Y	Y	
Galk1	Y	N	Y	Y		
Gas2l1	Y	N	Y	Y		
Gas6	Y	N	Y	Y		
Gas8	Y	N	Y	Y		
Gatm	Y	N	Y	Y		
Gcsh	Y	N	Y		Y	
Gdf11	Y	N	Y	Y		
Gdpd2	Y	N	Y	Y		
Gfod1	Y	N	Y			Y
Glb1	Y	N	Y	Y		
Gmpr2	Y	N	Y	Y		
Gna12	Y	N	Y			Y
Gnai2	Y	N	Y	Y		
Gng13	Y	N	Y			Y
Gng7	Y	N	Y	Y	Y	Y
Golga7b	Y	N	Y			Y
Gp1bb	Y	N	Y	Y		
Gpld1	Y	N	Y	Y		
Gpt	Y	N	Y	Y		
Grm3	Y	N	Y	Y		Y
Grm8	Y	N	Y	Y		
Gstm5	Y	N	Y	Y		
Gtf2e2	Y	N	Y	Y		
H2-D1	Y	N	Y	Y		
Hapln1	Y	N	Y		Y	Y
Hck	Y	N			Y	
Hdac5	Y	N	Y	Y		
Hells	Y	N	Y	Y		
Hemk1	Y	N	Y			Y
Hinfp	Y	N	Y	Y		

Gene name	Detected by Ex-ST?	Detected by ST?	Detected by downsampled Ex-ST?	Detected by Joshua, et al.?	Detected by Tushev, et al.?	Detected by Slide_seq V2?
Hipk1	Y	N	Y	Y		
Hipk2	Y	N	Y		Y	
Hira	Y	N	Y	Y		
Hist1h1b	Y	N			Y	
Hist1h1c	Y	N	Y	Y		
Hist1h1d	Y	N	Y		Y	
Hist1h2ac	Y	N	Y	Y		
Hist1h2ae	Y	N	Y	Y		
Hist1h2ap	Y	N			Y	
Hist1h2bc	Y	N	Y	Y		
Hmgb2	Y	N	Y	Y		
Hsd3b7	Y	N	Y	Y		
Hspb8	Y	N	Y	Y		
Id3	Y	N	Y	Y		
Id4	Y	N	Y	Y		
Idua	Y	N	Y	Y		
Ifi27	Y	N	Y	Y		
Igbp1	Y	N	Y	Y		
Igf2	Y	N	Y	Y		
Il33	Y	N		Y		
Il6st	Y	N	Y	Y		
Iqsec2	Y	N	Y	Y		
Iqsec3	Y	N	Y			Y
Irak1	Y	N	Y		Y	
Itpripl1	Y	N	Y		Y	
Jade1	Y	N	Y	Y		
Jagn1	Y	N	Y	Y		
Jph3	Y	N	Y			Y
Kcnj13	Y	N	Y		Y	
Kdm6b	Y	N	Y	Y		
Kif1c	Y	N	Y	Y		
Kifc2	Y	N	Y	Y		
Kirrel2	Y	N	Y		Y	
Kiss1r	Y	N	Y	Y		
Lamp2	Y	N	Y	Y		
Lars2	Y	N	Y	Y		
Lbr	Y	N	Y	Y		
Lca5	Y	N	Y	Y		
Limch1	Y	N	Y	Y		
Lims1	Y	N	Y	Y		

Gene name	Detected by Ex-ST?	Detected by ST?	Detected by downsampled Ex-ST?	Detected by Joshua, et al.?	Detected by Tushev, et al.?	Detected by Slide_seq V2?
Litaf	Y	N	Y	Y		
Lix1	Y	N	Y			Y
Lrch4	Y	N	Y	Y		
Lrp10	Y	N	Y	Y		
Ltbp1	Y	N	Y		Y	
Ly86	Y	N	Y	Y		
Mafg	Y	N	Y		Y	Y
Malat1	Y	N	Y	Y		
Map3k10	Y	N	Y	Y		
Marf1	Y	N	Y	Y		
Mars	Y	N	Y	Y		
Mbp	Y	N	Y	Y		
Mcl1	Y	N	Y	Y		
Med25	Y	N	Y	Y		
Mef2c	Y	N	Y		Y	
Meis2	Y	N	Y	Y		
Mfap1b	Y	N	Y	Y		
Mfap3l	Y	N	Y			Y
Mfge8	Y	N	Y		Y	
Mgat4b	Y	N	Y	Y		
Mgll	Y	N	Y	Y		Y
Mgmt	Y	N	Y	Y		
Mlst8	Y	N	Y	Y		
Mmp24	Y	N	Y			Y
Mn1	Y	N	Y	Y		
Mob1a	Y	N	Y	Y		
Mospd2	Y	N	Y	Y		
Mospd3	Y	N	Y	Y		Y
Mpdu1	Y	N	Y	Y		
Mpst	Y	N	Y	Y		
Mrc1	Y	N		Y		
Mreg	Y	N	Y	Y		
Msn	Y	N	Y	Y		
Mt3	Y	N	Y		Y	Y
mt-Atp6	Y	N	Y	Y		
Mturn	Y	N	Y	Y	Y	
Mvb12a	Y	N	Y	Y		
Mycbp	Y	N	Y	Y		
Myh9	Y	N	Y	Y		
Nadk2	Y	N	Y	Y		

Gene name	Detected by Ex-ST?	Detected by ST?	Detected by downsampled Ex-ST?	Detected by Joshua, et al.?	Detected by Tushev, et al.?	Detected by Slide_seq V2?
Nckap5	Y	N	Y	Y		
Ndrg1	Y	N	Y	Y		
Nenf	Y	N	Y	Y		
Nf2	Y	N	Y			Y
Nfkb2	Y	N	Y	Y		
Nme2	Y	N	Y	Y		
Nmral1	Y	N	Y	Y		
Nop2	Y	N	Y	Y		
Npc2	Y	N	Y	Y		
Nr2e1	Y	N	Y		Y	
Nsdhl	Y	N	Y	Y		
Nudc	Y	N	Y	Y		
Nup133	Y	N	Y	Y		
Oat	Y	N	Y	Y		
Oxa1l	Y	N	Y	Y		
P2ry12	Y	N	Y	Y		
Pabpc1	Y	N	Y	Y		
Palm	Y	N	Y	Y		
Panx2	Y	N	Y			Y
Pcdhgc5	Y	N			Y	
Pcsk6	Y	N	Y	Y		
Pctp	Y	N		Y		
Pcyt1b	Y	N	Y		Y	
Pdxdc1	Y	N	Y	Y		Y
Pdxk	Y	N	Y	Y		Y
Pdzd4	Y	N	Y	Y		
Phactr1	Y	N	Y			Y
Phc1	Y	N	Y	Y		
Phyh	Y	N	Y	Y		Y
Phyhipl	Y	N	Y	Y		
Pigq	Y	N	Y	Y		
Pigu	Y	N	Y	Y		
Pik3r1	Y	N	Y	Y		
Pink1	Y	N	Y	Y		
Pip5k1c	Y	N	Y		Y	
Pitpnm2	Y	N	Y	Y	Y	
Pknox1	Y	N	Y	Y		
Pla2g7	Y	N	Y	Y		
Plekhb2	Y	N	Y	Y		Y
Plekhm2	Y	N		Y		

Gene name	Detected by Ex-ST?	Detected by ST?	Detected by downsampled Ex-ST?	Detected by Joshua, et al.?	Detected by Tushev, et al.?	Detected by Slide_seq V2?
Plk3	Y	N	Y	Y		
Plk4	Y	N	Y	Y		
Plxnb1	Y	N	Y	Y		
Pnp	Y	N	Y	Y		
Pom121	Y	N	Y		Y	
Pomgnt1	Y	N	Y	Y		
Ppfia3	Y	N	Y	Y		
Ppp1r16a	Y	N	Y	Y		
Prcp	Y	N	Y	Y		
Prex1	Y	N		Y		
Prkaa2	Y	N	Y	Y		
Prkcd	Y	N	Y	Y		
Prr11	Y	N			Y	
Prr13	Y	N	Y	Y		
Prrc2a	Y	N		Y		
Psd2	Y	N	Y	Y		
Psme1	Y	N	Y	Y		
Ptp4a3	Y	N	Y	Y		
Ptpmt1	Y	N	Y		Y	
Ptpn1	Y	N	Y	Y		
Pycr1	Y	N			Y	
Pygb	Y	N	Y	Y		
Qars	Y	N	Y	Y		
Qdpr	Y	N		Y		
Rab11fip4	Y	N	Y		Y	Y
Rack1	Y	N	Y			Y
Rapgef4	Y	N	Y	Y		
Rasa3	Y	N	Y	Y		
Rasl10b	Y	N	Y	Y		
Rbck1	Y	N	Y	Y		
Rcan3	Y	N	Y	Y		
Reep6	Y	N	Y	Y		
Reln	Y	N	Y		Y	
Rftn2	Y	N		Y		
Rgs20	Y	N		Y		
Rhog	Y	N	Y	Y		
Rhoh	Y	N	Y	Y		
Rin2	Y	N	Y	Y		
Rmst	Y	N	Y	Y		
Rnf165	Y	N	Y			Y

Gene name	Detected by Ex-ST?	Detected by ST?	Detected by downsampled Ex-ST?	Detected by Joshua, et al.?	Detected by Tushev, et al.?	Detected by Slide_seq V2?
Rnf31	Y	N	Y	Y		
Rpia	Y	N	Y	Y		
Rpl27	Y	N	Y	Y		
Rplp0	Y	N	Y	Y		
Rps12	Y	N	Y	Y		
Rps13	Y	N	Y	Y		
Rps16	Y	N	Y	Y		
Rps2	Y	N	Y	Y		
Rps6ka4	Y	N	Y		Y	
Rsu1	Y	N	Y	Y		
Rtn2	Y	N	Y	Y		
Ryk	Y	N	Y	Y		
Samd4	Y	N	Y	Y		
Sbk1	Y	N	Y	Y		Y
Scaf1	Y	N		Y		
Scd1	Y	N	Y	Y		
Scd3	Y	N	Y	Y		
Scrt1	Y	N	Y			Y
Sdhc	Y	N	Y	Y		
Sec61a1	Y	N	Y	Y		
Serinc3	Y	N	Y	Y		
Serpine2	Y	N	Y	Y		
Setd3	Y	N	Y	Y		
Sft2d2	Y	N	Y	Y		
Sfxn1	Y	N	Y	Y		
Sgsm2	Y	N	Y	Y		
Sh2b1	Y	N	Y	Y		
Sh3glb1	Y	N	Y	Y		Y
Shank1	Y	N	Y			Y
Shank3	Y	N	Y			Y
Shc3	Y	N			Y	Y
Shisa4	Y	N		Y		
Sipa1l1	Y	N	Y			Y
Ski	Y	N	Y	Y		
Slamf9	Y	N			Y	
Slc12a2	Y	N	Y	Y		
Slc1a2	Y	N	Y	Y		Y
Slc1a3	Y	N	Y	Y		Y
Slc25a33	Y	N	Y	Y		
Slc38a3	Y	N	Y			Y

Gene name	Detected by Ex-ST?	Detected by ST?	Detected by downsampled Ex-ST?	Detected by Joshua, et al.?	Detected by Tushev, et al.?	Detected by Slide_seq V2?
Slc6a1	Y	N	Y	Y	Y	Y
Slc6a11	Y	N	Y			Y
Slc6a8	Y	N	Y	Y		
Slpi	Y	N		Y		
Smarcal1	Y	N	Y	Y		
Smarcc2	Y	N	Y	Y		Y
Smdt1	Y	N	Y		Y	Y
Smpdl3a	Y	N	Y	Y		
Snx9	Y	N	Y	Y		
Socs7	Y	N	Y	Y		
Sord	Y	N	Y	Y		
Spata13	Y	N	Y	Y		
Srcin1	Y	N	Y			Y
Srf	Y	N	Y	Y		
Stat3	Y	N	Y	Y		
Stk17b	Y	N	Y	Y		
Stk40	Y	N	Y	Y		
Stpg1	Y	N	Y	Y		
Stxbp5l	Y	N	Y		Y	
Suds3	Y	N	Y	Y		Y
Swap70	Y	N	Y	Y		
Syf2	Y	N	Y	Y		
Syn3	Y	N	Y	Y		
Taf9	Y	N	Y	Y		
Tbccd1	Y	N	Y	Y		
Tbkbp1	Y	N	Y			Y
Tdp1	Y	N	Y	Y		
Tdrd3	Y	N	Y	Y		
Tef	Y	N	Y		Y	
Thra	Y	N	Y	Y		Y
Tmem134	Y	N	Y	Y		
Tmem151b	Y	N	Y	Y		
Tmem160	Y	N	Y		Y	
Tmem185b	Y	N	Y	Y		
Tmem229a	Y	N	Y			Y
Tmpo	Y	N	Y	Y		
Tnfaip8l2	Y	N	Y	Y		
Tnrc18	Y	N	Y	Y		
Tor1aip1	Y	N	Y	Y		
Tprkb	Y	N	Y	Y		

Gene name	Detected by Ex-ST?	Detected by ST?	Detected by downsampled Ex-ST?	Detected by Joshua, et al.?	Detected by Tushev, et al.?	Detected by Slide_seq V2?
Trak1	Y	N	Y	Y		
Trim12a	Y	N	Y	Y		
Trim12c	Y	N	Y	Y		
Trim59	Y	N	Y	Y		
Trmt112	Y	N	Y	Y		
Trp53bp2	Y	N	Y	Y		
Trp53inp1	Y	N	Y	Y		
Tsen34	Y	N	Y	Y		
Ttc7b	Y	N	Y	Y		
Ttf1	Y	N	Y	Y		
Ttll3	Y	N	Y	Y		
Ttr	Y	N	Y		Y	
Tuba1c	Y	N	Y	Y		
Txnip	Y	N	Y	Y		
U2af1l4	Y	N	Y	Y		
Ubqln4	Y	N	Y	Y		Y
Ubxn7	Y	N	Y	Y		
Ucp2	Y	N	Y	Y		
Uqcr11	Y	N	Y	Y		Y
Usp21	Y	N	Y	Y		
Usp6nl	Y	N	Y	Y		
Vip	Y	N	Y		Y	
Wbp1	Y	N	Y	Y		
Wdr44	Y	N	Y	Y		
Wdr89	Y	N	Y	Y		
Wiz	Y	N	Y			Y
Xrcc5	Y	N	Y	Y		
Ybx1	Y	N	Y	Y	Y	
Yes1	Y	N	Y	Y		
Zadh2	Y	N	Y	Y		
Zbtb14	Y	N	Y	Y		
Zfp146	Y	N	Y		Y	
Zfp341	Y	N	Y	Y		
Zfp358	Y	N	Y	Y		
Zfp366	Y	N			Y	
Zfp367	Y	N	Y	Y		
Zfp568	Y	N	Y	Y		
Zfp574	Y	N	Y	Y		
Zfp664	Y	N	Y	Y		
Zfp703	Y	N	Y	Y		

Gene name	Detected by Ex-ST?	Detected by ST?	Detected by downsampled Ex-ST?	Detected by Joshua, et al.?	Detected by Tushev, et al.?	Detected by Slide_seq V2?
Zfp867	Y	N	Y	Y		
Zmiz2	Y	N	Y	Y		

Supplementary Material

Refer to Web version on PubMed Central for supplementary material.

Acknowledgements

We thank Y Lim, J Gibson and Z Zeng for critical discussions, and K Zhu and H Matsunami for sharing the data with us to validate the mapped glomeruli positions. YF is a Bio-X Stanford Interdisciplinary Graduate Fellow. CC is supported by a NSF Graduate Research Fellowship and a Stanford Graduate Fellowship. BW is a Beckman Young Investigator. This work is supported by an NIH grant (1R35GM138061) to BW, the Neuro-omics project of Wu Tsai Big Ideas in Neuroscience program to L Luo and BW, the European Research Council (ERC) under the European Union's Horizon 2020 research and innovation program (grant agreement no. 101021019) to JL, and Swedish Research council to JL.

Data availability

Mouse brain section containing hippocampus region is a publicly available dataset that can be found along with mouse reference genome mm10 on 10x Genomics website[26]. Single-cell RNAseq dataset of mouse brain can be downloaded online[27]. MOB bulk RNAseq and Slide-seq datasets used for comparison were obtained from references[11,12]. All data generated in this study (standard Visium data on MOB, all Ex-ST data, and Visium data generated using the modified protocol) including space ranger output files, stereoscope output files, DAPI and brightfield images are available at the Mendeley repository[28]. Raw sequence data can be found at NCBI BioProject with accession number PRJNA957091.

References

1. Larsson L, Frisén J & Lundeberg J Spatially resolved transcriptomics adds a new dimension to genomics. Nat. Methods 18, 15–18 (2021). [PubMed: 33408402]
2. Rao A, Barkley D, França GS & Yanai I Exploring tissue architecture using spatial transcriptomics. Nature 596, 211–220 (2021). [PubMed: 34381231]
3. Moses L & Pachter L Museum of spatial transcriptomics. Nat. Methods 19, 534–546 (2022). [PubMed: 35273392]
4. Ståhl PL et al. Visualization and analysis of gene expression in tissue sections by spatial transcriptomics. Science 353, 78–82 (2016). [PubMed: 27365449]
5. Asp M et al. A Spatiotemporal organ-wide gene expression and cell atlas of the developing human heart. Cell 179, 1647–1660.e19 (2019). [PubMed: 31835037]
6. Lewis SM et al. Spatial Omics and multiplexed imaging to explore cancer biology. Nat. Methods 18, 997–1012 (2021). [PubMed: 34341583]
7. Maniatis S et al. Spatiotemporal dynamics of molecular pathology in amyotrophic lateral sclerosis. Science 364, 89–93 (2019). [PubMed: 30948552]
8. Wassie AT, Zhao Y & Boyden ES Expansion microscopy: principles and uses in biological research. Nat. Methods 16, 33–41 (2019). [PubMed: 30573813]

9. Tepe B et al. Single-cell RNA-Seq of mouse olfactory bulb reveals cellular heterogeneity and activity-dependent molecular census of adult-born neurons. Cell Rep. 25, 2689–2703.e3 (2018). [PubMed: 30517858]
10. Allen Institute for Brain Science (2004). Allen Mouse Brain Atlas. Mouse.brain-map.org.
11. Endo F, et al. Molecular basis of astrocyte diversity and morphology across the CNS in health and disease. Science 378, eadc9020 (2022). [PubMed: 36378959]
12. Rodriques SG, et al. Slide-seq: A scalable technology for measuring genome-wide expression at high spatial resolution. Science 363, 1463–1467 (2019). [PubMed: 30923225]
13. Andersson A et al. Single-cell and spatial transcriptomics enables probabilistic inference of cell type topography. Commun. Biol 3, 565 (2020). [PubMed: 33037292]
14. Ressler KJ, Sullivan SL & Buck LB Information coding in the olfactory system: evidence for a stereotyped and highly organized epitope map in the olfactory bulb. Cell 79, 1245–1255 (1994). [PubMed: 7528109]
15. Vassar R et al. Topographic organization of sensory projections to the olfactory bulb. Cell 79, 981–991 (1994). [PubMed: 8001145]
16. Zeisel A et al. Molecular architecture of the mouse nervous system. Cell 174, 999–1014.e22 (2018). [PubMed: 30096314]
17. Kosik KS Life at low copy number: How dendrites manage with so few mRNAs. Neuron 92, 1168–1180 (2016). [PubMed: 28009273]
18. Stickels RR et al. Highly sensitive spatial transcriptomics at near-cellular resolution with Slide-seqV2. Nat. Biotechnol 39, 313–319 (2021). [PubMed: 33288904]
19. Tushev G et al. Alternative 3' UTRs modify the localization, regulatory potential, stability, and plasticity of mRNAs in neuronal compartments. Neuron 98, 495–511.e6 (2018). [PubMed: 29656876]
20. Ainsley JA, Drane L, Jacobs J, Kittelberger KA & Reijmers LG Functionally diverse dendritic mRNAs rapidly associate with ribosomes following a novel experience. Nat. Commun 5, 4510 (2014). [PubMed: 25072471]
21. Chen A et al. Spatiotemporal transcriptomic atlas of mouse organogenesis using DNA nanoball-patterned arrays. Cell 185, 1777–1792.e21 (2022). [PubMed: 35512705]
22. Zhu KW et al. Decoding the olfactory map through targeted transcriptomics links murine olfactory receptors to glomeruli. Nat. Commun 13, 5137 (2022). [PubMed: 36050313]
23. Moffitt JR et al. High-performance multiplexed fluorescence in situ hybridization in culture and tissue with matrix imprinting and clearing. Proc. Natl. Acad. Sci. U. S. A 113, 14456–14461 (2016). [PubMed: 27911841]
24. Fan Y et al. Mechanical expansion microscopy. Methods Cell Biol. 161, 125–146 (2021). [PubMed: 33478686]
25. Tarashansky AJ, Xue Y, Li P, Quake SR & Wang B Self-assembling manifolds in single-cell RNA sequencing data. eLife 8, e48994 (2019). [PubMed: 31524596]
26. https://www.10xgenomics.com/resources/datasets/mouse-brain-section-coronal-1-standard-1-0-0
27. http://mousebrain.org/adolescent/downloads.html
28. Andrusivova Z & Fan Y Ex-ST, Mendeley Data, v1, 10.17632/nrbsxrk9mp.1

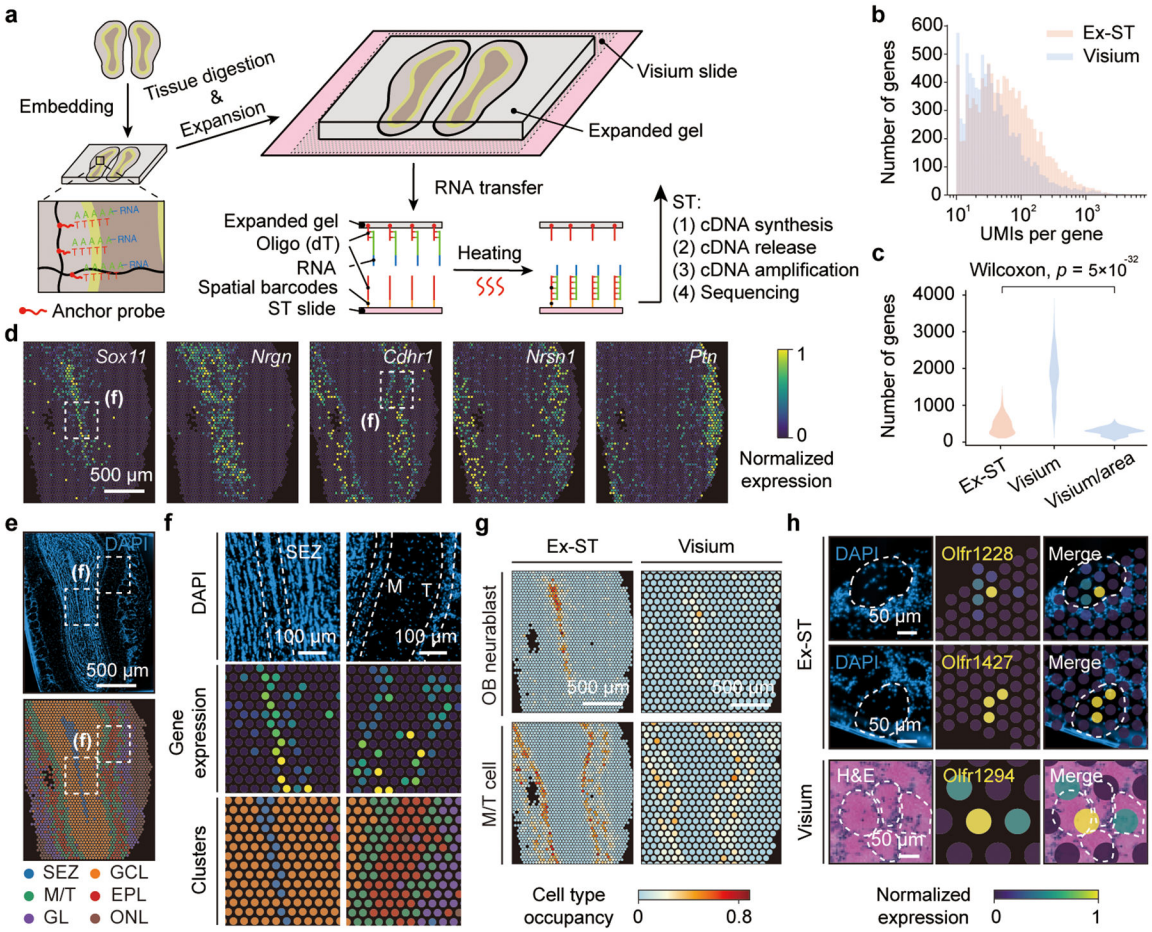

Fig. 1: Ex-ST resolves MOB layers with high resolution.

a, Overview of the Ex-ST workflow. **b,** Comparison of number of UMIs for all genes present in the Ex-ST and standard Visium datasets, each containing two MOB sections. **c,** Violin plot showing the number of genes per spot measured by Ex-ST, standard Visium, and standard Visium after normalizing the tissue area covering each spot. *P* value: two-sided, two-sample Mann-Whitney-Wilcoxon tests. **d,** Spatially resolved expression of region-specific marker genes processed by the Ex-ST protocol. **e,** DAPI image of expanded MOB section (top) and annotated clusters on tissue coordinates (bottom): SEZ, subependymal zone; GCL, granular layer; M/T, mitral and tufted cell layer; EPL, external plexiform layer; GL, glomerular layer; ONL, olfactory nerve layer. **f,** Magnified views of SEZ and M/T regions processed by Ex-ST. Top: DAPI images with SEZ and M/T regions with dashed outlines; middle: expression of region-specific marker genes (*Sox11* for SEZ and *Cdhr1* for M/T region); bottom: cluster labels mapped on tissue coordinates. **g,** Comparison of cell type occupancy of each spot in the Ex-ST and standard Visium data visualized for two cell types, OB neuroblasts and M/T cells. **h,** Expression of olfactory receptors (Olfr) in both Ex-ST and standard Visium datasets. DAPI (Ex-ST) and HE (standard Visium) images showing the locations of glomeruli with boundaries indicated by dashed lines. The localization of Olfr, detected by Ex-ST, in specific glomeruli is in agreement with coordinates provided by a previous study using serial sectioning[22]. Since Ex-ST and standard Visium datasets

were produced using different MOB specimens, different Olfrs are captured. Scale bars for expanded samples in all panels have been rescaled by the expansion ratio.

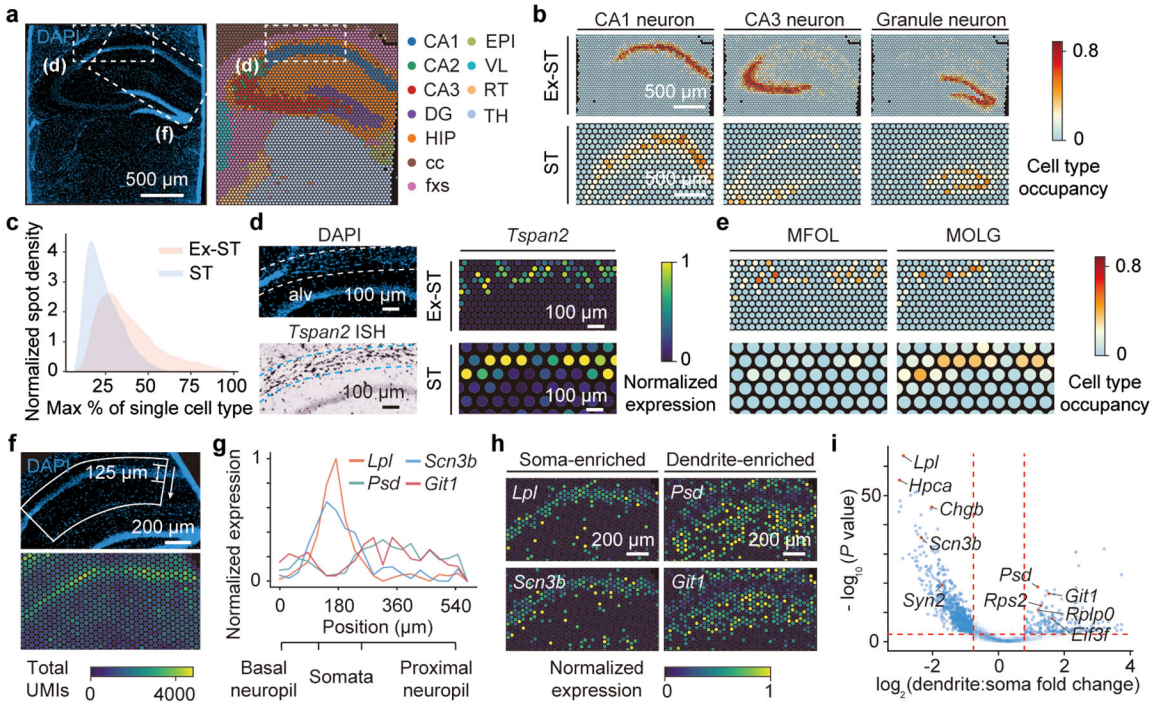

Fig. 2: Ex-ST dissects fine structures in the mouse hippocampus.

a, DAPI image of an expanded mouse hippocampus section (left) and annotated clusters on tissue coordinates (right): CA1–3, hippocampal subfields; DG, dentate gyrus; HIP, hippocampal region; cc, corpus callosum; fxs, fornix system; EPI, epithalamus; VL, lateral ventricle; RT, reticular nucleus of the thalamus; TH, thalamus. **b,** Comparison of cell type composition of individual spots in the Ex-ST and standard Visium data visualized for three cell types. **c,** Occupancy of dominating cell type in each spot of both the Ex-ST and standard Visium data visualized as a density plot. **d,** Magnified DAPI image showing the sporadic distribution of cell bodies in alveus (top left; alv, dashed outlines). ISH of *Tspan2* showing oligodendrocyte cell bodies, obtained from Allen brain atlas (bottom left)[10]. Comparison of normalized *Tspan2* expression in the Ex-ST and standard Visium data (right). **e,** Comparison of cell type composition of individual spots in the Ex-ST and standard Visium data visualized for oligodendrocyte subclasses. **f,** Magnified DAPI image showing the high nuclear density within the CA1 region (top). Spatial distribution of UMI counts within the CA1 region (bottom). **g,** Expression profiles of soma-dendrite differentially expressed genes along the axis indicated in **f**. **h,** Normalized spatial expression of soma-enriched and dendrite-enriched genes. **i,** Volcano plot showing differential gene expression between soma and dendritic regions. *P* values: two-sided, two-sample Mann-Whitney-Wilcoxon tests. Gene with $\log_2$ (fold change) > 0.8 and *P* value < 0.001 (dashed lines) are considered differentially expressed. Several previously known soma- and dendrite-enriched genes are specified. Scale bars for expanded samples in all panels have been rescaled by the expansion ratio.